Inertial Sensing with Quantum Gases

Thomas Arne Hensel, Sina Loriani, Christian Schubert et. al.
Gottfried Wilhelm Leibniz University Hannover
Welfengarten 1
30167 Hannover
GERMANY

Thomas.hensel@mpinat.mpg.de

ABSTRACT

Light-pulse atom interferometers that use quantum sensors have the capability to measure inertial and electromagnetic forces with high precision. These sensors are essential for determining fundamental constants like the fine structure constant and testing foundational laws of modern physics such as the equivalence principle. The accuracy of these sensors is maximized with long interrogation times and large momentum transfer. In this study[1,2], we demonstrate the benefits of using Bose-Einstein condensed sources for precision interferometry when dealing with challenging conditions. We compare the systematic and statistical effects of using Bose-Einstein condensed sources with thermal sources in three cases related to Earth- and space-based sensors. The outcomes of this research have the potential to contribute to the development of next-generation inertial measurement units.

1.0 INTRODUCTION

Atom interferometers find application in both inertially sensitive measurements and diverse fundamental physics tests. Enhancing sensitivity involves transferring numerous photons during beam-splitting, extending free fall duration while preserving contrast and atomic flux. Meanwhile, accurate error characterization demands increased control over atom manipulation and preparation. Theoretical and experimental investigations address limitations of interferometers with molasses-cooled atoms and their alleviation by reducing residual expansion rates.

In this study, we evaluate the suitability of two atomic ensemble regimes for precision tests, considering the trade-off between flux and expansion rate. We analyze factors including shot noise, cycle times, excitation rates, and major systematics such as gravity gradients (GGs), Coriolis force, wave-front aberrations (WFA), and mean-field interactions.

Space mission proposals primarily rely on Delta-Kick collimation (DKC) using optical or magnetic potentials to capitalize on extended microgravity free fall periods. This approach achieves minimal wave packet expansion rates equivalent to pK temperatures in thermal ensembles. Bose-Einstein-condensed (BEC) ensembles are better suited for DKC, especially for extended interrogation times. However, they face reduced atomic flux due to evaporation, despite recent promising studies. In contrast, molasses-cooled atoms have more atoms, yet their typical 1D velocity filtering leads to a lower atom flux, as we elaborate in our study.

To exemplify our comparative study between condensed and thermal sources, we explore three key scenarios for free-fall atom interferometers: a gravimeter, gravity-gradiometer, and test of the universality of free fall (also known as the Weak Equivalence Principle (WEP) test) (see Figure 1 for a visual representation). In this study, thermal sources refer to atomic ensembles with negligible condensed fraction, while BEC sources possess a 100% condensed fraction. For each scenario, we constrain the maximum atomic ensemble diameter during recombination to maintain contrast. This constraint facilitates calculating shot noise and other error terms to assess the trade-off.

2.0 RESULTS

In general, the performance of an atom interferometric Inertial Measurement Unit (IMU) depends on parameters such as the effective momentum transfer (denoted by k_{eff}), the interrogation time (T), number of available atoms and achievable contrast among others. The quantity one aims to measure is a phase, which depends on a parameter of interest. For a gravimeter, the phase scales as $\phi \propto k_{eff} g T^2$ proportional to strength of the gravitational field g, whereas $\phi \propto k_{eff} D \Gamma T^2$ for gradiometers with separation D and gravity gradient Γ.

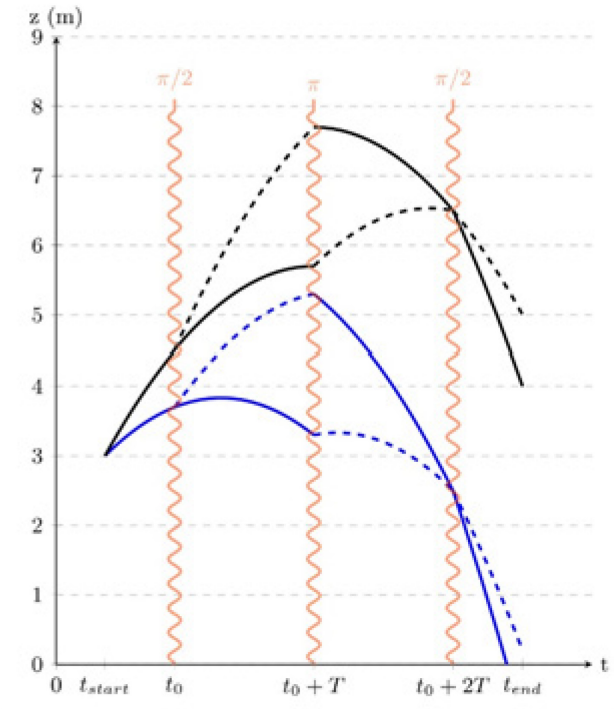

Figure 1: The gradiometer geometry comprises two Mach-Zehnder (MZ) sequences, each represented by black and blue lines. These MZ sequences start with an initial separation of D at the first beam splitter. Each MZ sequence involves three successive light pulses, which include a beam splitter (first π/2-pulse), a mirror (π-pulse), and a merging beam splitter after 2T. Dashed lines signify internal state changes caused by momentum transfer from atom-light interactions. A single MZ sequence corresponds to a gravimeter sequence for measuring the gravitational field coupling constant g of one species. Using two MZ sequences operated with distinct species enables the determination of η for a WEP test. In that case, the differential velocity at t = t_{start} for the MZ sequences is adjusted to ensure spatial overlap, eliminating the impact of gravity gradients while retaining sensitivity to potential species-specific differential acceleration.

Assuming shot-noise-limited measurements, a fixed atom number, and no reduction in contrast, increasing free evolution time T or effective momentum transfer can enhance single-shot phase sensitivity. In general, the advantage of a larger number of atoms in thermal ensembles reduces shot noise. Their larger spatial extension is expected to efficiently mitigate mean-field effects compared to BECs. Conversely, the same position and velocity distributions could limit achievable scaling factors due to systematic uncertainties and atom losses.

Beyond shot noise considerations, an array of physical phenomena act as limiting factors for precision experiments by interacting with the velocity spread or spatial extension of the ensemble. These phenomena include the Coriolis effect, gravity gradients, wave-front aberrations, and mean-field effects. We quantify various systematic and statistical effects that could constrain forthcoming experiments beyond current capabilities, such as long-fountain atomic gravimeters, space-based atom interferometers, and ground-based lab atom interferometers in microgravity conditions. In the following, we present the key findings of the study - for an in-depth discussion, the interested reader is referred to[1].

The three specific cases chosen for comparison involve advanced inertial sensors that could surpass current capabilities in the near future: (i) a ground-based gravimeter[3] aiming for a relative uncertainty of $\Delta g/g = 10^{-9}$, (ii) a space gradiometer targeting a 2.5 mE resolution[4], and (iii) a WEP-test with an uncertainty of 2×10^{-15} in determining the Eötvös ratio[5]. The interferometer geometries are depicted in Figure 1. To assess the performance of each regime, we will employ typical parameters for thermal ensembles and BECs and evaluate their outcomes in the three experiments. Specifics regarding initial parameters and all results are displayed in Table 1.

Systematic effects arising from GGs and the Coriolis force are contingent on uncertainties in the initial mean position (δr) and velocity (δv) at the onset of the interferometry sequence. The number of measurements (ν_0) necessary for their characterization is determined for each application to ensure that the most substantial systematic phase uncertainty associated with GGs or rotations remains below the chosen target uncertainty for the respective measurement.

In general, various effects S (gravity gradients, rotations, light wave front distortions) couple to the atomic source characteristics q (initial position and velocity, density), leading to additional phase shifts. In case of a gravimeter, for example, $\phi_S = k_{eff} T^2 \times Sq$, and a potential phase contribution$\phi_\gamma = k_{eff} T^2 \gamma z_0$ is given by gravity gradients $S = \gamma$ that couple to the initial position $q = z_0$ of an atom at the first pulse of the interferometric sequence. In the assessment of the sensor performance, the influence of the uncertainties δS, δq on the phase is evaluated by quantifying the derived uncertainties $\delta\phi_S = S\delta q, q\delta S$ and $\delta S \delta q$. The uncertainties can be of different origin, and in the following we will continuously use δ to denote systematic (bias) uncertainties and σ for statistical uncertainties.

As a specific example: $\delta_{\phi,\gamma} = k_{\mathrm{eff}} T^2 z_0 \delta_\gamma$ and $k_{\mathrm{eff}} T^2 \gamma \delta_{z_0}$ are systematic phase uncertainties due to limited knowledge about the values of γ and z_0, whereas $\sigma_{\phi,\gamma} = k_{\mathrm{eff}} T^2 \gamma \sigma_{z_0}$ is a statistical uncertainty, given by the statistical distribution of the atomic position around the mean z_0, quantified by the standard deviation σ_{z_0}. The important difference is that the systematic contributions have to be controlled at the target accuracy level, which can be achieved through pre-interferometry characterization measurements (e.g., accurate determination of the mean position reduces δz) or by minimizing the coupling factor S. The statistical uncertainty, on the other hand, is reduced by repeated measurements, i.e., realizations of the atom interferometer.

The prerequisite number of experiments needed to mitigate systematic effects to the desired level might differ between the BEC and thermal cases. Thermal ensembles have more atoms and are larger than BECs after DKC. This reduces the minimally required number of measurements of the thermal ensemble by a factor of 2-5. For the sake of comparability, we choose to compute all systematic effects using ν_0 of the BEC case, enabling an assessment of performance with a consistent set of parameters.

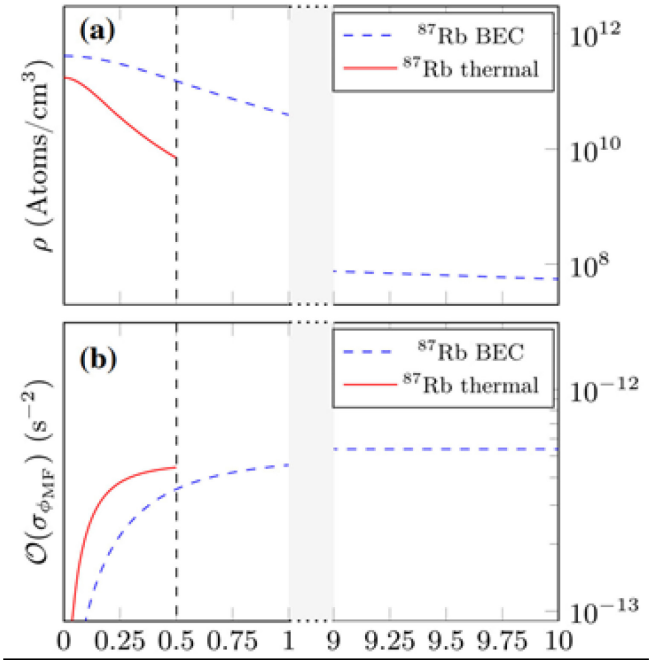

Figure 2: Atomic densities and time averaged mean-field statistical uncertainty for the space-gradiometer scenario. a) Time-dependent density ρ of the ensembles during the interferometer time based on a DKC sequence. b) Fractional statistical phase uncertainty due to mean-field effects integrated over a number of n_{cycle} experiments.

The systematic phase uncertainty arising from WFA results from the limited knowledge (δR) about the wave-front curvature of the beam splitter and is given by $\phi_{WFA} \propto \frac{k_{eff}}{R}\frac{k_B T_{at}}{m_{at}}T^2$. Statistical fluctuations $\sigma_{T_{at}}$ in the effective temperature lead to a phase noise $\sigma_{\phi_{WFA}} = \frac{k_{eff}T^2 k_B}{m_{at}R}\sigma_{T_{at}}$, whereas limited knowledge δR about the wave front curvature results in a systematic uncertainty $\delta_{\phi_{WFA}} = \frac{k_{eff}T^2 T_{at} k_B}{m_{at}R^2}\,\delta_R$. To simplify subsequent considerations, we assume that the wave-front curvature (R) and its uncertainty (δR) are of comparable magnitude. In contrast, statistical uncertainty due to temperature fluctuations is negligible, assuming these fluctuations are of the same order of magnitude as the ensemble's effective temperature.

Mean-field effects arise due to atom–atom interactions in atomic ensembles, scale with growing densities and are an additional source for statistical errors. The mean-field energy reads $E_{MF}(r) = g_{int}n(r)$ and depends on the local density $n(r)$ of the ensemble and the interaction strength g_{int}. We take the average of the mean-field energy by weighting it with the respective density distribution to calculate spurious a phase shift associated with mean-field effects due to an imperfect balance of atoms in the two arms of the interferometer. If the initial beam splitter creates a superposition that deviates by b from equal probability in both states, the phase shift $\phi_{MF}(t) = \frac{b}{\hbar}\int_0^t \langle E_{MF}(r(t'))\rangle dt'$ occurs, corresponding to the integral of the differential frequency shift between the arms.

Two of the most relevant effects are related to GGs and the Coriolis force. The first is the acceleration uncertainty due to the mass distribution of Earth and the apparatus surrounding the experiment. The second arises due to the transverse motion of the atoms with respect to the incident beam in combination with Earth's rotation. Both give rise to additional phase shifts as they couple to the initial kinematic conditions of the ensemble (velocity and spatial spread).

To adjust statistical error contributions like shot noise and mean-field effects to the desired precision for each measurement type, we calculate the minimum number of iterations n_{cycle} required to attain the target uncertainty. For a straightforward comparison between BEC and thermal ensemble performance differences, the integration time remains consistent across both regimes, initially established by the number of cycles needed to mitigate BEC's statistical effects below the target level. As thermal sources can be generated with shorter preparation times, more cycles can be conducted within the same integration time. To estimate various uncertainties, ensemble properties such as spatial and velocity spreads are calculated at each atom-light interaction pulse, factoring in the spatial and velocity selectivity of the pulses. Modified spatial and velocity spreads are utilized as evaluation inputs for mean-field effects, WFA, and contrast estimation.

Eventually, the main limitations in all cases are systematic effects, e.g. WFA, which cannot be reduced by increasing integration time or number of measurement cycles. Additionally, the strong expansion of the thermal ensembles compared to that of BECs causes two drawbacks that counteract the benefit of high initial atom numbers. First, larger ensemble diameters significantly reduce the contrast at the output port, which increases shot noise. Second, the different expansion behaviour of thermal ensemble and BEC causes mean field effects to rise to a similar level in the thermal case on relevant time scales (see Figure 1, Table 1).

Table 1: Estimation of statistical and systematic uncertainties for three scenarios: a lab-based 87Rb gravimeter, a space-borne 87Rb gradiometer and a satellite 87Rb/41K WEP-test analogous to the STE-QUEST mission.

Parameter\case	Gravimeter		Gradiometer		WEP-test	
	Thermal	BEC	Thermal	BEC	Thermal	BEC
N_{at} (initial)	1×10^9	1×10^6	1×10^9	1×10^6	1×10^9	1×10^6
T_{at} (K)	80×10^{-9}	50×10^{-12}	80×10^{-9}	50×10^{-12}	80×10^{-9}	50×10^{-12}
P_{exc}	0.57	0.99	0.33	0.97	0.43	0.99
t_{int} (s); n_{cycle}	3.36; 7	3.45; 3	86400; 72000	86400; 4320	2×10^7; 2.4×10^7	2×10^7; 10^6
ν_0	1		50		10^6	
2T (s)	150×10^{-3}		0.5	10	0.5	10
$\mathcal{O}(\delta_{\phi_{target}})$	$\Delta g/g = 10^{-9}$		$\Gamma = 2.5$ mE$= 2.5 \times 10^{-12}$ s^{-2}		$\eta = 2 \times 10^{-15}$	
$\mathcal{O}(\sigma_{\phi_{SN}})$	1.2×10^{-11}	3.3×10^{-10}	5.0×10^{-13} s^{-2}	5.5×10^{-14} s^{-2}	1.2×10^{-15}	2.1×10^{-16}
$\mathcal{O}(\delta_{\phi_{GG}})$	4.9×10^{-15}	1.1×10^{-14}	2.4×10^{-14} s^{-2}	9.9×10^{-13} s^{-2}	1.1×10^{-17}	4.8×10^{-16}
$\mathcal{O}(\delta_{\phi_C})$	1.8×10^{-14}	3.7×10^{-14}	7.0×10^{-14} s^{-2}	1.5×10^{-13} s^{-2}	3.7×10^{-17}	7.6×10^{-17}
$\mathcal{O}(\delta_{\phi_{WFA}})$	3.4×10^{-10}	2.1×10^{-13}	1.0×10^{-12} s^{-2}	4.4×10^{-15} s^{-2}	1.3×10^{-12}	8.0×10^{-16}
$\mathcal{O}(\sigma_{\phi_{MF}})$	1.3×10^{-11}	9.2×10^{-10}	4.7×10^{-13} s^{-2}	5.4×10^{-13} s^{-2}	1.1×10^{-15}	1.8×10^{-15}

3.0 CONCLUSION

Our study implies that thermal sources hold advantages in scenarios where moderate scale factors or rapid readouts are required, benefiting from shorter cycle times and larger atom numbers. However, this advantage diminishes when transitioning from short to extended interferometry times, surpassing current standards.

Across our study cases, BEC-based scenarios demonstrate comparable shot-noise levels and mean-field effects to thermal sources, given equal integration time. Optimistically, we anticipate thermal ensembles could be collimated to the 80 nK level, achieving similar efficiency in preparing, transporting, and engineering quantum states as BECs. Notably, BECs still exhibit significantly higher contrast (close to 1) compared to thermal ensembles. Additionally, thermal ensembles face a critical limit imposed by WFA, incompatible with extended interrogation times crucial for advanced applications. In contrast, BEC ensembles, with their compact sizes, present a limit at least three orders of magnitude lower, showcasing their metrological potential.

Although this study does not consider small-scale distortions of optical beams, which could imply an apparent BEC disadvantage due to averaging effects for WFA, the ability to engineer a BEC's size mitigates this concern. The flexibility in adjusting initial size allows for tailored analysis of WFA with varying periodicities. The trade-off between size-stretch-induced phase uncertainties, such as balancing GGs or Coriolis systematics against WFA effects, becomes feasible, especially when gravity gradient compensation schemes are considered.

In conclusion, for relatively short interferometry times (a few hundred milliseconds), both thermal and BEC sources yield comparable performance. However, for extended durations, BEC sources distinctly excel, as size-related systematic effects are orders of magnitude smaller than those of thermal ensembles.

4.0 REFERENCES

[1] Hensel, T. et al. Inertial sensing with quantum gases: a comparative performance study of condensed versus thermal sources for atom interferometry. Eur. Phys. J. D 75, 108 (2021).

[2] Ahlers, H. et al. STE-QUEST: Space Time Explorer and QUantum Equivalence principle Space Test. arXiv:2211.15412 (2022).

[3] Louchet-Chauvet, A. et al. The influence of transverse motion within an atomic gravimeter. New J. Phys. 13, 065025 (2011).

[4] Trimeche, A. et al. Concept study and preliminary design of a cold atom interferometer for space gravity gradiometry. Class. Quantum Grav. 36, 215004 (2019).

[5] Aguilera, D. N. et al. STE-QUEST—test of the universality of free fall using cold atom interferometry. Class. Quantum Grav. 31, 115010 (2014).